



# Synthesis and photophysics of platinum(II) complexes bearing 2-(7-(4-*R*-phenylethynyl)-9,9-dihexadecyl-fluoren-2-yl)-1,10-phenanthroline ligand

Xu-Guang Liu, Wenfang Sun\*

Department of Chemistry and Biochemistry, North Dakota State University, Fargo, ND 58108-6050, USA

## ARTICLE INFO

### Article history:

Received 31 December 2011  
Received in revised form 10 March 2012  
Accepted 19 March 2012  
Available online 27 March 2012

### Keywords:

Electronic absorption  
Emission  
2-(7-(4-*R*-Phenylethynyl)-9,9-dihexadecyl-fluoren-2-yl)-1,10-phenanthroline  
Platinum complexes  
Transient absorption

## ABSTRACT

A series of platinum(II) complexes bearing 2-(7-(4-*R*-phenylethynyl)-9,9-dihexadecyl-fluoren-2-yl)-1,10-phenanthroline ligand were synthesized and characterized. Their photophysical properties were systematically investigated by UV–Vis absorption, emission, and transient absorption spectroscopy. All complexes exhibit  $^1\pi,\pi^*$  absorption bands below 410 nm and charge transfer transitions at 415–550 nm in  $\text{CH}_2\text{Cl}_2$ . They all emit at ca. 624 nm with vibronic structures. Both UV–Vis absorption and emission spectra show negative solvatochromic effect. All complexes exhibit broad and moderately strong triplet transient absorption from the near-UV to the near-IR spectral region. Reverse saturable absorption of these complexes in  $\text{CH}_2\text{Cl}_2$  for ns laser pulses at 532 nm was demonstrated.

© 2012 Elsevier B.V. All rights reserved.

## 1. Introduction

Square-planar platinum(II) terdentate complexes have attracted great attention in the past two decades due to their unique photophysical properties, such as room-temperature phosphorescence and broadband excited-state absorption. Most importantly, these properties can be readily tuned via structural modifications to tailor the specific requirements for different applications. It has been reported that Pt(II) terdentate complexes can be potentially used in light-emitting devices [1], chemosensors [2], chemical cells for hydrogen generation [3], solar cells [4], and nonlinear optical devices [5]. Among the Pt(II) terdentate complexes studied, Pt(II) complexes containing aromatic N-donor (such as pyridine) and/or cyclometalated (such as benzene) ligands are discovered to display multiple charge-transfer excited states, including metal-to-ligand charge transfer (MLCT), ligand-to-ligand charge transfer (LLCT), intraligand charge transfer (ILCT), and intra-/inter-molecular metal-metal-to-ligand charge transfer (MMLCT). A number of Pt complexes exhibiting moderate charge-transfer absorption in the visible spectral region and relatively long-lived charge-transfer emission at room temperature in solutions have been reported [6]. Among which, platinum complexes bearing 6-phenyl-2,2'-bipyridine ligand ( $C^{\wedge}N^{\wedge}N$ ) are particularly interesting because of their

relatively intense emission at room temperature compared to the platinum terpyridyl complexes [7]. This feature is attributed to the stronger  $\pi$ -donating ability of the phenyl ring, which admixes the ILCT character into the lowest excited state, and to the reduced distortion of the square-planar configuration around the Pt ion by the  $C^{\wedge}N^{\wedge}N$  ligand, which decreases the nonradiative decay from the excited state.

An earlier study by Che's group revealed that by increasing the  $\pi$ -conjugation of the  $C^{\wedge}N^{\wedge}N$  ligand, the structural distortion of the triplet excited state is minimized; consequently the phosphorescence quantum yield was improved [1c,8]. Our group recently reported the photophysics and nonlinear absorption of platinum(II) complexes with 4-fluorenyl substituent on the  $C^{\wedge}N^{\wedge}N$  ligand, which enhanced the triplet excited-state lifetime, improved the emission quantum yield, and increased the ratios of the excited-state absorption cross-section to that of the ground-state [9]. Che's group also reported that by incorporating fluorene component to the  $C^{\wedge}N^{\wedge}N$  ligand, the emission quantum yield of Pt(II) complexes could be increased up to 0.76 [10]. It appears that extending the  $\pi$ -conjugation of the  $C^{\wedge}N^{\wedge}N$  ligand could significantly influence the excited-state properties of the Pt(II) complexes.

1,10-Phenanthroline has been reported to be a useful chelating bidentate ligand for transition metal ions [11]. Compared to the 2,2'-bipyridine and 2,2';6',6''-terpyridine ligands, the rigidity of phenanthroline holds the nitrogen donor atoms juxtaposed and thus favors metal binding. Recently Andraud's group reported the

\* Corresponding author. Tel.: +1 701 231 6254; fax: +1 701 231 8831.  
E-mail address: [Wenfang.Sun@ndsu.edu](mailto:Wenfang.Sun@ndsu.edu) (W. Sun).

two-photon induced excited-state absorption of novel 5-(oligofluorenyl)-1,10-phenanthroline ligands and their Ru complexes [12]. However, the synthesis and utilization of 2-fluorenyl-1,10-phenanthroline as a new type of C<sup>N</sup>N ligand for Pt(II) have not been reported in the literature. Considering the rigidity of the phenanthroline component and the possibility of extending the  $\pi$ -conjugation via introducing substituted phenylethynyl group at the 7-position of the fluorenyl ring, we anticipate that the emission quantum yield and the lifetime of the triplet excited state of the Pt complex incorporating this ligand could be increased. To verify this hypothesis, we designed and synthesized a series of platinum(II) complexes bearing 2-(7-(4-R-phenylethynyl)-9,9-dihexadecanylfluoren-2-yl)-1,10-phenanthroline ligand (complexes **5a–5d** in Scheme 1). Different electron donating- or accepting-group was introduced on the phenyl ring to understand how these auxiliary substituents influence the photophysics of the complexes.

## 2. Experimental

### 2.1. Synthesis

#### 2.1.1. General procedures and materials

All of the starting compounds (fluorene, 4-substituted phenylacetylene (**2**), etc.) and solvents were purchased from Alfa Aesar or Aldrich Chemical Co., and the solvents were used as is unless otherwise stated. The precursor 8-amino-7-quinolinecarbaldehyde was prepared according to the literature procedures [13]. The intermediates were characterized by NMR, while the final platinum complexes were fully characterized by <sup>1</sup>H NMR, <sup>13</sup>C NMR, electrospray ionization high resolution mass spectrometry (ESI-HRMS), and elemental analyses.

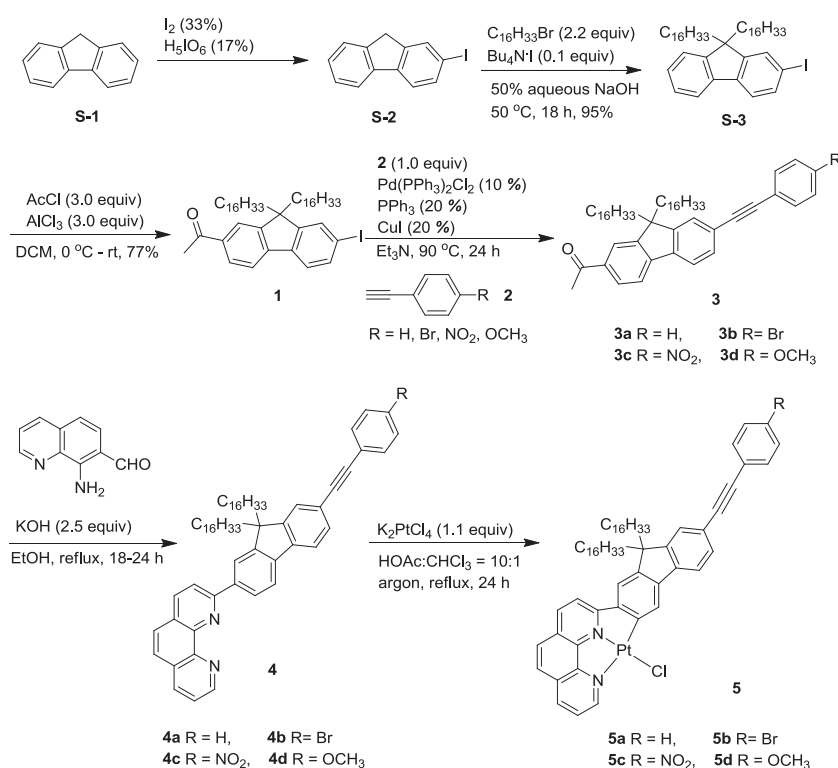
NMR spectra were obtained on a Varian-Oxford 400 VNMR or a Varian Oxford-500 VNMR spectrometer. ESI-HRMS analyses were conducted on a Bruker Daltonics BioTOF III mass spectrometer. Elemental analyses were carried out by NuMega Resonance Laboratories, Inc., San Diego, California.

The synthetic route for platinum(II) complexes **5a–5d** is outlined in Scheme 1, and the synthetic details and characterization data for the ligands and the complexes are provided below. Precursor **1** was prepared according to the literature procedures [14] via iodination of fluorene, then alkylation of the 2-iodofluorene, and acetylation of the alkylated 2-iodofluorene. After that, Sonogashira cross-coupling reaction of **1** and 4-substituted phenylacetylene (**2**) leads to compound **3**. Ligands **4a–4d** were then obtained through the Friedländer condensation reaction between **4** and 8-aminoquinoline-7-carbaldehyde. Finally, the platinum(II) complexes were obtained by reacting K<sub>2</sub>PtCl<sub>4</sub> with the corresponding ligands under reflux in mixed acetic acid/chloroform (V/V = 10/1) solution [10]. Due to the long alkyl chains at the fluorene motif, these cyclometalated platinum(II) complexes exhibit good solubility in common organic solvents, which is important for the photophysical studies and potential applications.

#### 2.1.2. Synthesis of precursor **1**

**2.1.2.1. 2-Iodofluorene (S-2).** Fluorene (0.10 mol, 16.60 g) was dissolved in 167 ml boiling solvent of AcOH/H<sub>2</sub>O/H<sub>2</sub>SO<sub>4</sub> (V:V:V = 100:20:3). After that, the reaction mixture was cooled down to 100 °C, and periodic acid dehydrates (0.017 mol, 3.80 g) and iodine (0.033 mol, 8.46 g) were added. The reaction mixture was further cooled down to 70 °C and stirred at this temperature for 4 h until the elementary iodine almost disappeared and precipitates were formed. After cooling down to room temperature, the pale yellow solid was collected by filtration and washed with saturated aqueous Na<sub>2</sub>CO<sub>3</sub> and water several times. The crude product was purified by recrystallization from hexane to give 14.0 g pale yellow solid (yield = 48%). <sup>1</sup>H NMR (400 MHz, CDCl<sub>3</sub>):  $\delta$  3.84 (s, 2H, CH<sub>2</sub>), 7.28–7.37 (m, 2H, Ar), 7.49–7.52 (m, 2H), 7.65–7.68 (m, 1H), 7.73 (d, *J* = 7.2 Hz, 1H, Ar), 7.85–7.86 (m, 1H, Ar).

**2.1.2.2. 9,9-Dihexadecyl-2-iodo-9H-fluorene (S-3).** 2-Iodofluorene (**S-2**, 10.0 mmol, 2.92 g) and tetra-*n*-butylammonium iodine (1.0 mmol, 369 mg) were dissolved in 18 ml of DMSO and 7 ml of



**Scheme 1.** Synthetic route for platinum(II) complexes **5a–5d**.

50% aqueous NaOH. 1-Bromohexadecane (22 mmol, 6.71 g) was then added in the solution. The reaction mixture was stirred at 50 °C under argon for 18 h; and was then diluted with ethyl acetate. The organic layer was washed with dilute HCl twice and brine twice, and was dried over anhydrous Na<sub>2</sub>SO<sub>4</sub>. The resultant oil was purified by flash chromatography (silica gel) with hexane used as the eluent. <sup>1</sup>H NMR (400 MHz, CDCl<sub>3</sub>): δ 0.85 (t, *J* = 7.2 Hz, 6H, CH<sub>3</sub>), 1.01–1.29 (m, 56H, CH<sub>2</sub>), 1.81–1.93 (m, 4H, CH<sub>2</sub>), 7.28–7.31 (m, 3H, Ar), 7.41 (d, *J* = 8.4 Hz, 1H, Ar), 7.60–7.64 (m, 3H, Ar).

**2.1.2.3. Dihexadecyl-7-iodo-9H-fluoren-2-yl)ethanone (1) [14].** Acetyl chloride (224 μl, 3.15 mmol, 247 mg) was slowly added at 0 °C to a suspension of anhydrous AlCl<sub>3</sub> (3.60 mmol, 480 mg) in dry CH<sub>2</sub>Cl<sub>2</sub> (10 ml). A CH<sub>2</sub>Cl<sub>2</sub> solution of 9,9-dihexadecyl-2-iodo-9H-fluorene (3.00 mmol, 2.22 g) was added dropwise and the mixture was stirred at room temperature for 18 h. The reaction mixture was poured onto ice and a concentrated HCl aqueous solution was added until the precipitate of Al(OH)<sub>3</sub> dissolved. The organic layer was separated and the aqueous phase was extracted twice with CH<sub>2</sub>Cl<sub>2</sub>. The organic phases were combined, washed with water, 2% NaOH solution, water, brine, and dried over Na<sub>2</sub>SO<sub>4</sub>. After evaporation of the solvent, the oil obtained was purified by flash chromatography (silica gel, with hexane to hexane/ethyl acetate = 75:1–30:1–15:1 used as the eluent). 1.80 g white solid was obtained (yield = 77%). <sup>1</sup>H NMR (400 MHz, CDCl<sub>3</sub>): δ 0.52–0.54 (m, 4H, CH<sub>2</sub>), 0.84 (t, *J* = 6.4 Hz, 6H, CH<sub>3</sub>), 0.86–1.27 (m, 52H, CH<sub>2</sub>), 1.89–1.98 (m, 4H, CH<sub>2</sub>), 2.63 (s, 3H, CH<sub>3</sub>), 7.45–7.48 (m, 1H, Ar), 7.65–7.71 (m, 3H, Ar), 7.90–7.93 (m, 2H, Ar). <sup>13</sup>C NMR (100 MHz, CDCl<sub>3</sub>): δ 14.1, 22.7, 23.7, 26.8, 29.2, 29.3, 29.5, 29.57, 29.63, 29.8, 31.9, 40.0, 55.5, 94.3, 119.6, 122.2, 122.4, 128.2, 132.3, 136.1, 136.3, 139.4, 144.9, 150.5, 154.2, 197.8.

### 2.1.3. Synthesis of 3 using Sonogashira cross-coupling reaction

**2.1.3.1. General procedure for Sonogashira cross-coupling reaction.** Compounds **1** (1.0 equiv.), **2** (1.0 equiv.), Pd(PPh<sub>3</sub>)Cl<sub>2</sub> (0.10 equiv.), PPh<sub>3</sub> (0.20 equiv.), and CuI (0.20 equiv.) were added to a round-bottom flask. The flask was evacuated and backfilled with argon. Et<sub>3</sub>N (15 ml) was then added. The reaction mixture was heated at reflux for 24 h; and then was allowed to cool down to room temperature. After removal of the solvent, the residue was extracted with CH<sub>2</sub>Cl<sub>2</sub>, and the CH<sub>2</sub>Cl<sub>2</sub> layer was washed with water and brine and dried over anhydrous Na<sub>2</sub>SO<sub>4</sub>. The solvent was then removed and the crude product was purified by column chromatography (silica gel) with hexane/ethyl acetate used as eluent.

**3a.** 320 mg yellow solid, yield: 85%. <sup>1</sup>H NMR (400 MHz, CDCl<sub>3</sub>): δ 0.55–0.57 (m, 4H, CH<sub>2</sub>), 0.85 (t, *J* = 6.0 Hz, 6H, CH<sub>3</sub>), 1.01–1.27 (m, 52H, CH<sub>2</sub>), 1.93–2.05 (m, 4H, CH<sub>2</sub>), 2.64 (s, 3H, CH<sub>3</sub>), 7.32–7.34 (m, 3H, Ar), 7.52–7.56 (m, 4H, Ar), 7.71 (t, *J* = 6.8 Hz, 2H, Ar), 7.93–7.95 (m, 2H, Ar). <sup>13</sup>C NMR (100 MHz, CDCl<sub>3</sub>): δ 14.1, 22.7, 23.7, 26.8, 29.2, 29.3, 29.52, 29.57, 29.6, 29.9, 31.9, 40.2, 55.4, 90.2, 119.7, 120.6, 122.4, 123.0, 123.2, 126.1, 128.2, 128.3, 128.34, 130.8, 131.6, 136.1, 139.9, 145.2, 151.3, 152.0, 197.9. ESI-MS: *m/z* calcd for C<sub>55</sub>H<sub>80</sub>O [M+Na<sup>+</sup>], 779.6107; found, 779.6094.

**3b.** 370 mg yellow solid, yield: 86%. <sup>1</sup>H NMR (400 MHz, CDCl<sub>3</sub>): δ 0.56–0.58 (m, 4H, CH<sub>2</sub>), 0.87 (t, *J* = 6.8 Hz, 6H, CH<sub>3</sub>), 1.02–1.28 (m, 52H, CH<sub>2</sub>), 1.94–2.05 (m, 4H, CH<sub>2</sub>), 2.66 (s, 3H, CH<sub>3</sub>), 7.40–7.43 (m, 2H, Ar), 7.47–7.54 (m, 4H, Ar), 7.71–7.75 (m, 2H, Ar), 7.94–7.97 (m, 2H, Ar). <sup>13</sup>C NMR (100 MHz, CDCl<sub>3</sub>): δ 14.1, 22.7, 23.7, 26.8, 29.2, 29.3, 29.5, 29.58, 29.63, 29.9, 31.9, 40.1, 55.4, 89.1, 91.3, 119.8, 120.7, 122.2, 122.4, 122.6, 126.1, 128.2, 130.8, 131.7, 133.0, 136.2, 140.2, 145.1, 151.3, 152.1, 197.9. ESI-MS: *m/z* calcd for C<sub>55</sub>H<sub>79</sub>OBr<sup>81</sup> [M+Na<sup>+</sup>], 859.5368; found, 859.6055.

**3c.** 290 mg yellow solid, yield: 72%. <sup>1</sup>H NMR (500 MHz, CDCl<sub>3</sub>): δ 0.54–0.55 (m, 4H), 0.82–0.86 (t, *J* = 6.4 Hz, 6H), 1.00–1.23 (m, 52H), 1.96–2.02 (m, 4H), 2.65 (s, 3H), 7.53–7.56 (m, 2H), 7.68 (d,

*J* = 8.8 Hz, 2H), 7.54 (d, *J* = 8.4 Hz, 2H), 7.94–7.96 (m, 2H), 8.22 (d, *J* = 8.8 Hz, 2H). <sup>13</sup>C NMR (100 MHz, CDCl<sub>3</sub>): δ 14.1, 22.7, 23.8, 26.9, 29.2, 29.3, 29.53, 29.59, 29.6, 29.9, 31.9, 40.1, 55.5, 88.3, 95.6, 120.0, 120.8, 121.6, 122.4, 123.7, 126.4, 128.3, 130.2, 131.2, 132.2, 136.4, 141.0, 144.9, 147.0, 151.5, 152.2, 197.9. ESI-MS: *m/z* calcd for C<sub>55</sub>H<sub>79</sub>NO<sub>3</sub> [M+2H<sup>+</sup>], 803.6211; found, 803.5492.

**3d.** 370 mg yellow solid, yield: 94%. <sup>1</sup>H NMR (400 MHz, CDCl<sub>3</sub>): δ 0.56–0.61 (m, 4H, CH<sub>2</sub>), 0.87 (t, *J* = 6.8 Hz, 6H, CH<sub>3</sub>), 1.02–1.30 (m, 52H, CH<sub>2</sub>), 1.97–2.04 (m, 4H, CH<sub>2</sub>), 2.66 (s, 3H, CH<sub>3</sub>), 3.83 (s, 3H, OCH<sub>3</sub>), 6.87–6.91 (m, 2H, Ar), 7.49–7.53 (m, 4H, Ar), 7.70–7.74 (m, 2H, Ar), 7.94–7.96 (m, 2H, Ar). <sup>13</sup>C NMR (100 MHz, CDCl<sub>3</sub>): δ 14.1, 22.7, 23.7, 26.8, 29.2, 29.3, 29.52, 29.57, 29.6, 29.9, 31.9, 40.2, 55.2, 55.4, 88.9, 90.2, 114.0, 115.3, 119.7, 120.6, 122.4, 123.3, 125.9, 128.2, 130.6, 133.0, 136.0, 139.6, 145.3, 151.3, 152.0, 159.7, 197.9. ESI-MS: *m/z* calcd for C<sub>56</sub>H<sub>82</sub>O<sub>2</sub> [M+Na<sup>+</sup>], 809.6213; found, 809.6186.

### 2.1.4. Synthesis of ligands 4a–4d

**2.1.4.1. Typical procedure for Friedländer condensation [15].** A mixture of 8-aminoquinoline-7-carbaldehyde (1.0 equiv.), **3** (1.1 equiv.) and KOH (2.5 equiv.) in absolute EtOH was refluxed for 18–24 h under argon and cooled to room temperature. The solvent was evaporated under vacuum and the residue was extracted with ethyl acetate. The organic phase was washed with water for three times and dried over anhydrous Na<sub>2</sub>SO<sub>4</sub>. After removal of the solvent, the residue was purified by column chromatography (neutral Al<sub>2</sub>O<sub>3</sub> gel) with hexane/ethyl acetate used as the eluent.

**Ligand 4a:** 266 mg yellow oil, yield: 78%. <sup>1</sup>H NMR (400 MHz, CDCl<sub>3</sub>): δ 0.67–0.70 (m, 4H, CH<sub>2</sub>), 0.86 (t, *J* = 6.8 Hz, 6H, CH<sub>3</sub>), 1.05–1.29 (m, 52H, CH<sub>2</sub>), 2.02–2.16 (m, 4H, CH<sub>2</sub>), 7.32–7.38 (m, 3H, Ar), 7.55–7.60 (m, 4H, Ar), 7.61–7.64 (dd, *J*<sub>1</sub> = 4.4 Hz, *J*<sub>2</sub> = 8.0 Hz, 1H, Ar), 7.74–7.82 (m, 3H, Ar), 7.87 (d, *J* = 8.0 Hz, 1H, Ar), 8.13–8.16 (m, 2H, Ar), 8.24 (dd, *J*<sub>1</sub> = 1.6 Hz, *J*<sub>2</sub> = 8.0 Hz, 1H, Ar), 8.30 (dd, *J*<sub>1</sub> = 4.4 Hz, *J*<sub>2</sub> = 8.4 Hz, 1H, Ar), 8.45 (dd, *J*<sub>1</sub> = 1.6 Hz, *J*<sub>2</sub> = 8.0 Hz, 1H, Ar), 9.25 (dd, *J*<sub>1</sub> = 1.6 Hz, *J*<sub>2</sub> = 4.0 Hz, 1H, Ar). <sup>13</sup>C NMR (100 MHz, CDCl<sub>3</sub>): δ 14.1, 22.7, 23.8, 29.3, 29.56, 29.59, 29.6, 30.0, 31.9, 40.5, 55.4, 89.5, 09.6, 120.1, 120.5, 121.1, 121.7, 121.9, 122.9, 123.5, 126.0, 126.2, 126.4, 127.5, 127.8, 128.1, 128.3, 129.1, 130.7, 131.6, 136.0, 136.7, 139.3, 141.0, 141.7, 146.2, 146.4, 150.4, 151.4, 151.5, 158.1. ESI-MS: *m/z* calcd for C<sub>65</sub>H<sub>84</sub>N<sub>2</sub> [M+H<sup>+</sup>], 893.6713; found, 893.6718. *Anal. Calc.* for C<sub>65</sub>H<sub>84</sub>N<sub>2</sub> + H<sub>2</sub>O: C, 85.66; H, 9.51; N, 3.07. Found: C, 85.72; H, 9.10; N, 3.17%.

**Ligand 4b:** 238 mg yellow solid, yield: 78%. <sup>1</sup>H NMR (400 MHz, CDCl<sub>3</sub>): δ 0.67–0.70 (m, 4H, CH<sub>2</sub>), 0.86 (t, *J* = 6.4 Hz, 6H, CH<sub>3</sub>), 1.05–1.27 (m, 52H, CH<sub>2</sub>), 2.05–2.17 (m, 4H, CH<sub>2</sub>), 7.42–7.44 (m, 2H, Ar), 7.48–7.51 (m, 2H, Ar), 7.53–7.55 (m, 2H, Ar), 7.64 (dd, *J*<sub>1</sub> = 4.4 Hz, *J*<sub>2</sub> = 8.0 Hz, 1H, Ar), 7.74–7.83 (m, 3H, Ar), 7.87 (d, *J* = 8.0 Hz, 1H, Ar), 8.14–8.16 (m, 2H, Ar), 8.25 (d, *J* = 8.0 Hz, 1H, Ar), 8.32 (d, *J* = 8.4 Hz, 1H, Ar), 8.46 (d, *J* = 8.0 Hz, 1H, Ar), 9.25–9.26 (m, 1H, Ar). <sup>13</sup>C NMR (100 MHz, CDCl<sub>3</sub>): δ 14.1, 22.6, 23.8, 29.3, 29.5, 29.6, 30.0, 31.9, 40.4, 55.4, 88.5, 91.8, 120.1, 120.5, 121.1, 121.3, 121.9, 122.3, 122.4, 122.9, 125.9, 126.2, 126.3, 127.4, 127.8, 129.0, 130.7, 131.6, 132.9, 136.0, 136.7, 139.4, 141.3, 141.6, 146.2, 146.4, 150.4, 151.4, 151.5, 158.0. ESI-MS: *m/z* calcd for C<sub>65</sub>H<sub>83</sub>Br<sup>79</sup>N<sub>2</sub> [M+H<sup>+</sup>], 971.5818; found, 971.6057. *Anal. Calc.* for C<sub>65</sub>H<sub>83</sub>BrN<sub>2</sub>: C, 80.30; H, 8.60; N, 2.88. Found: C, 80.13; H, 8.38; N, 2.86%.

**Ligand 4c:** 186 mg yellow solid, yield: 60%. <sup>1</sup>H NMR (400 MHz, CDCl<sub>3</sub>): δ 0.65–0.67 (m, 4H, CH<sub>2</sub>), 0.82 (t, *J* = 6.8 Hz, 6H, CH<sub>3</sub>), 1.02–1.23 (m, 52H, CH<sub>2</sub>), 2.01–2.17 (m, 4H, CH<sub>2</sub>), 7.53–7.55 (m, 2H, Ar), 7.60 (dd, *J*<sub>1</sub> = 4.0 Hz, *J*<sub>2</sub> = 8.0 Hz, 1H, Ar), 7.65 (d, *J* = 8.8 Hz, 2H, Ar), 7.71–7.78 (m, 3H, Ar), 7.86 (d, *J* = 8.0 Hz, 1H, Ar), 8.12 (d, *J* = 8.4 Hz, 1H, Ar), 8.17–8.29 (m, 4H, Ar), 8.28 (d, *J* = 8.4 Hz, 1H, Ar), 8.42 (d, *J* = 8.4 Hz, 1H, Ar), 9.20–9.21 (m, 1H). <sup>13</sup>C NMR (100 MHz, CDCl<sub>3</sub>): δ 14.0, 22.6, 23.8, 29.2, 29.5, 29.6,

29.9, 31.8, 40.3, 55.5, 87.8, 96.1, 120.2, 120.4, 120.6, 120.9, 121.9, 122.8, 123.5, 126.12, 126.16, 126.3, 127.4, 127.7, 129.0, 130.4, 131.0, 132.0, 136.0, 136.7, 139.6, 141.3, 142.0, 146.0, 146.3, 146.7, 150.2, 151.5, 151.6, 157.8, ESI-MS:  $m/z$  calcd for  $C_{65}H_{83}N_3O_2$ ,  $[M+H^+]$  938.6558; found, 938.6519. Anal. Calc. for  $C_{65}H_{83}N_3O_2$ : C, 83.20; H, 8.92; N, 4.48. Found: C, 82.72; H, 8.67; N, 4.43%.

**Ligand 4d**: 191 mg yellow solid, yield: 59%.  $^1H$  NMR (400 MHz,  $CDCl_3$ ):  $\delta$  0.66–0.68 (m, 4H,  $CH_2$ ), 0.86 (t,  $J = 6.8$  Hz, 6H,  $CH_3$ ), 1.04–1.29 (m, 52H,  $CH_2$ ), 1.99–2.16 (m, 4H,  $CH_2$ ), 3.83 (s, 3H,  $OCH_3$ ), 6.90 (d,  $J = 8.8$  Hz, 2H, Ar), 7.51–7.55 (m, 4H, Ar), 7.64 (dd,  $J_1 = 4.4$  Hz,  $J_2 = 8.0$  Hz, 1H, Ar), 7.73–7.87 (m, 4H, Ar), 8.13–8.17 (m, 2H, Ar), 8.25 (dd,  $J_1 = 2.0$  Hz,  $J_2 = 8.0$  Hz, 1H, Ar), 8.32 (d,  $J = 8.4$  Hz, 2H, Ar), 8.45 (dd,  $J_1 = 1.6$  Hz,  $J_2 = 8.0$  Hz, 1H, Ar), 9.25 (dd,  $J_1 = 1.6$  Hz,  $J_2 = 4.4$  Hz, 1H, Ar).  $^{13}C$  NMR (100 MHz,  $CDCl_3$ ):  $\delta$  14.1, 22.6, 23.8, 29.3, 29.5, 29.6, 30.0, 31.9, 40.5, 55.2, 55.4, 89.3, 89.5, 114.0, 115.5, 120.0, 120.4, 121.1, 121.8, 122.1, 122.9, 125.8, 126.1, 126.3, 127.4, 127.8, 129.1, 130.5, 133.0, 136.0, 136.7, 139.2, 140.7, 141.8, 146.2, 146.4, 150.4, 151.4, 151.5, 158.1, 159.6. ESI-MS:  $m/z$  calcd for  $C_{66}H_{86}N_2O$ ,  $[M+H^+]$  923.6818; found, 923.6839. Anal. Calc. for  $C_{66}H_{86}N_2O$ : C, 85.85; H, 9.39; N, 3.03. Found: C, 85.48; H, 9.02; N, 3.10%.

## 2.1.5. Synthesis of platinum complexes 5a–5d

**2.1.5.1. General procedure for complexation [10]**. A mixture of **4** (1.00 equiv.) and  $K_2PtCl_4$  (1.25 equiv.) in chloroform and acetic acid mixture (V:V = 1:10) was refluxed for 24 h under argon. The orange solid was filtered, washed with water and diethyl ether several times.

**Complex 5a**: 90 mg orange solid, yield: 43%.  $^1H$  NMR (500 MHz,  $CDCl_3$ ):  $\delta$  0.77–0.87 (m, 10H,  $CH_2 + CH_3$ ), 1.11–1.27 (m, 52H,  $CH_2$ ), 2.01–2.09 (m, 4H,  $CH_2$ ), 7.33–7.40 (m, 4H, Ar), 7.53–7.69 (m, 8H, Ar), 7.86 (d,  $J = 8.0$  Hz, 1H, Ar), 8.00–8.05 (m, 2H, Ar), 8.32 (d,  $J = 8.0$  Hz, 1H, Ar), 8.89–8.91 (m, 1H, Ar).  $^{13}C$  NMR (100 MHz,  $CDCl_3$ ):  $\delta$  14.1, 22.6, 24.0, 29.3, 29.5, 29.6, 30.2, 31.9, 40.7, 54.9, 89.8, 90.6, 118.1, 119.4, 121.0, 122.1, 123.5, 125.6, 125.7, 125.9, 126.6, 126.7, 126.8, 128.2, 128.4, 130.8, 130.9, 131.6, 136.2, 137.0, 141.0, 141.3, 144.2, 145.2, 145.9, 146.7, 147.5, 149.2, 151.5, 165.2. ESI-MS:  $m/z$  calcd for  $C_{65}H_{83}ClN_2Pt$ ,  $[M+Na^+]$  1144.5790; found, 1144.5787. Anal. Calc. for  $C_{65}H_{83}ClN_2Pt$ : C, 69.53; H, 7.45; N, 2.49. Found: C, 69.89; H, 7.34; N, 2.50%.

**Complex 5b**: 72 mg orange solid, yield: 33%.  $^1H$  NMR (400 MHz,  $CDCl_3$ ):  $\delta$  0.71–0.87 (m, 10H,  $CH_2 + CH_3$ ), 1.10–1.28 (m, 52H,  $CH_2$ ), 1.99–2.08 (m, 4H,  $CH_2$ ), 7.32 (s, 1H, Ar), 7.44 (d,  $J = 8.4$  Hz, 2H, Ar), 7.50–7.52 (m, 3H, Ar), 7.55–7.68 (m, 5H, Ar), 7.85 (d,  $J = 7.6$  Hz, 1H, Ar), 8.00 (s, 1H, Ar), 8.04 (d,  $J = 8.0$  Hz, 1H, Ar), 8.31 (d,  $J = 7.6$  Hz, 1H, Ar), 8.88 (d,  $J = 4.4$  Hz, 1H, Ar).  $^{13}C$  NMR (100 MHz,  $CDCl_3$ ):  $\delta$  14.1, 22.6, 24.0, 29.3, 29.4, 29.6, 30.2, 31.9, 40.5, 54.9, 88.8, 91.8, 118.2, 119.4, 121.1, 121.7, 122.3, 122.5, 125.7, 125.9, 126.6, 126.7, 130.8, 130.9, 131.6, 132.9, 136.3, 137.0, 140.9, 141.5, 144.1, 145.3, 145.9, 146.7, 147.6, 149.2, 151.6, 165.2. ESI-MS:  $m/z$  calcd for  $C_{65}H_{82}BrClN_2Pt$ ,  $[M+Na^+]$  1222.4895; found, 1222.4891. Anal. Calc. for  $C_{65}H_{82}BrClN_2Pt$ : C, 64.92; H, 6.88; N, 2.33. Found: C, 64.92; H, 6.72; N, 2.39%.

**Complex 5c**: 83 mg orange solid, yield: 44%.  $^1H$  NMR (500 MHz,  $CDCl_3$ ):  $\delta$  0.76–0.86 (m, 10H,  $CH_2 + CH_3$ ), 1.11–1.25 (m, 52H,  $CH_2$ ), 2.05–2.07 (m, 4H,  $CH_2$ ), 7.33 (s, 1H, Ar), 7.55–7.65 (m, 6H, Ar), 7.72 (d,  $J = 8.5$  Hz, 2H, Ar), 7.87 (d,  $J = 7.5$  Hz, 1H, Ar), 7.99–8.02 (m, 2H, Ar), 8.25 (d,  $J = 8.5$  Hz, 2H, Ar), 8.30 (d,  $J = 8.0$  Hz, 1H, Ar), 8.83 (d,  $J = 4.5$  Hz, 1H, Ar).  $^{13}C$  NMR (100 MHz,  $CDCl_3$ ):  $\delta$  14.1, 22.6, 24.1, 29.3, 29.4, 29.5, 29.6, 30.2, 31.8, 40.5, 54.9, 88.1, 96.2, 118.2, 119.4, 120.8, 121.1, 123.7, 125.8, 125.9, 126.6, 126.7, 126.8, 130.5, 130.9, 131.2, 132.2, 136.3, 137.1, 141.1, 142.3, 143.7, 145.6, 145.8, 146.7, 146.8, 147.5, 149.1, 151.7, 164.9. ESI-MS:  $m/z$  calcd for  $C_{65}H_{82}ClN_3O_2Pt$ ,  $[M+Na^+]$  1189.5641; found, 1189.5648.

Anal. Calc. for  $C_{65}H_{82}ClN_3O_2Pt$ : C, 66.85; H, 7.08; N, 3.60. Found: C, 66.38; H, 6.88; N, 3.51%.

**Complex 5d**: 80 mg orange solid, yield: 50%.  $^1H$  NMR (500 MHz,  $CDCl_3$ ):  $\delta$  0.78–0.87 (m, 10H,  $CH_2 + CH_3$ ), 1.10–1.27 (m, 52H,  $CH_2$ ), 2.00–2.08 (m, 4H,  $CH_2$ ), 3.86 (s, 3H,  $OCH_3$ ), 6.92 (d,  $J = 7.0$  Hz, 2H, Ar), 7.32 (s, 1H, Ar), 7.51–7.68 (m, 8H, Ar), 7.85 (d,  $J = 8.0$  Hz, 1H, Ar), 8.00–8.05 (m, 2H, Ar), 8.32 (d,  $J = 8.0$  Hz, 1H, Ar), 8.90 (d,  $J = 3.0$  Hz, 1H, Ar).  $^{13}C$  NMR (100 MHz,  $CDCl_3$ ):  $\delta$  14.1, 22.6, 24.0, 29.3, 29.5, 29.6, 30.2, 31.9, 40.6, 54.8, 55.3, 89.3, 89.8, 114.0, 115.6, 118.1, 119.4, 121.0, 122.5, 125.5, 125.6, 125.9, 126.5, 126.6, 126.7, 130.6, 130.9, 133.0, 136.2, 137.0, 141.0, 140.9, 144.3, 145.1, 145.9, 146.7, 147.5, 149.2, 151.5, 159.6, 165.3. ESI-MS:  $m/z$  calcd for  $C_{66}H_{85}ClN_2OPt$ ,  $[M+Na^+]$  1174.5896; found, 1174.5884. Anal. Calc. for  $C_{66}H_{85}ClN_2OPt$ : C, 68.76; H, 7.43; N, 2.43. Found: C, 68.38; H, 7.06; N, 2.47%.

## 2.2. Photophysical measurements

The UV–Vis absorption spectra were acquired on an Agilent 8453 spectrophotometer in different HPLC-grade solvents. The steady-state emission spectra were recorded on a SPEX fluoro-log-3 fluorometer/phosphorometer in different solvents.

The emission quantum yields of the platinum complexes were determined by a comparative method in degassed solutions [16], in which a degassed aqueous solution of  $[Ru(bpy)_3]Cl_2$  ( $\Phi_{em} = 0.042$ ,  $\lambda_{ex} = 436$  nm) was used as the reference [17]. The excited-state lifetimes, the triplet excited-state quantum yields, and the triplet transient difference absorption spectra were measured in degassed solutions on an Edinburgh LP920 laser flash photolysis spectrometer. The third harmonic output (355 nm) of a Nd:YAG laser (Quantel Brilliant, pulsewidth  $\sim 4.1$  ns, repetition rate was set at 1 Hz) was used as the excitation source. Each sample was purged with argon for at least 30 min before measurement.

The self-quenching rate constants ( $k_q$ ) in dichloromethane were deduced following the Stern–Volmer equation,

$$k_{obs} = k_q[c] + k_0 \quad (1)$$

where  $k_{obs}$  is the measured radiative decay rate constant of the emission ( $k_{obs} = 1/\tau_{em}$ ) at a given concentration,  $k_q$  is the self-quenching rate constant,  $[c]$  is the concentration of the complex in mol/L, and  $k_0$  ( $k_0 = 1/\tau_0$ ) is the decay rate constant of the excited state at infinite dilute solution. A plot of the observed decay rate constant versus concentration should give rise to a straight line. The slope of the straight line corresponds to  $k_q$  and the intercept corresponds to  $k_0$ .

The triplet excited-state absorption coefficient ( $\epsilon_T$ ) at the absorption band maximum was measured by the singlet depletion method [18], in which the optical density changes during transient absorption at the minimum of the bleaching band ( $\Delta OD_S$ ) and the maximum of the positive band ( $\Delta OD_T$ ) were monitored.  $\epsilon_T$  was then calculated using the following equation [18]:

$$\epsilon_T = \frac{\epsilon_S \times \Delta OD_T}{\Delta OD_S} \quad (2)$$

where  $\epsilon_S$  is the ground-state molar extinction coefficient at the electronic absorption band maximum.

The quantum yield of the triplet excited state formation ( $\Phi_T$ ) was determined using the comparative method [19]. SiNc in benzene ( $\Phi_T = 0.20$ ,  $\epsilon_{T,590} = 70000$   $M^{-1} cm^{-1}$ ) [20] was used as the reference. All the solutions were optically matched at the excitation wavelength (355 nm), and the  $\Phi_T$  was calculated using equation [19]:

$$\Phi_T^s = \Phi_T^{ref} \times \frac{\Delta OD_T^s}{\Delta OD_T^{ref}} \times \frac{\epsilon_T^{ref}}{\epsilon_T^s} \quad (3)$$

where  $\Delta OD_T^s$  and  $\Delta OD_T^{ref}$  are the maximum optical density change during transient absorption due to triplet-triplet transition of the

sample and the reference, respectively;  $\varepsilon_T^{\text{ref}}$  and  $\varepsilon_T^s$  are the molar extinction coefficients of this transition at the wavelength where  $\Delta\text{OD}_T$  is measured for the reference and the sample, respectively.  $\Phi_T^{\text{ref}}$  is the triplet excited state quantum yield of the reference.

### 2.3. Nonlinear transmission measurements

The experimental setup was similar to what had been described previously [21]. The light source was the second harmonic output ( $\lambda = 532$  nm) of a 4.1 ns (fwhm), 10 Hz, Q-switched Quantel Brilliant Nd:YAG laser. A  $f = 30$  cm plano-convex lens was used to focus the laser beam to the center of a 2-mm-thick sample cuvette. The radius of the beam waist was  $\sim 75$   $\mu\text{m}$ . Two Molectron J4-09 pyroelectric probes and an EPM2000 energy/power meter were used to monitor the incident and output energies.

## 3. Results and discussion

### 3.1. Electronic absorption

The UV–Vis absorption of **5a–5d** were studied in  $\text{CH}_2\text{Cl}_2$  solutions at different concentrations ( $1 \times 10^{-6}$ – $5 \times 10^{-4}$  mol/L). The absorption of all complexes obeys Beer's law in the concentration range studied, indicating that no ground-state aggregation occurs in this concentration range (see inset in Fig. 1b) due to the presence of long alkyl chains at the fluorenyl component, which prevents aggregation. The UV–Vis absorption spectra of **5a–5d** are shown in Fig. 1b and the band maxima and molar extinction coefficients are listed in Table 1. All complexes exhibit intense structured absorption bands between 350 and 415 nm, which are red-shifted with respect to other reported cyclometalated  $\text{C}^{\wedge}\text{N}^{\wedge}\text{N}$  platinum (II) complexes [5a,9,10], and to the major absorption band of their respective ligand (Fig. 1a). Considering the large extinction coefficients of these bands and the similar energy to those of their corresponding ligands, we attribute these absorption bands to the  ${}^1\pi,\pi^*$  transitions within the  $\text{C}^{\wedge}\text{N}^{\wedge}\text{N}$  ligand. The red-shift of these bands with respect to those of their ligands implies the interactions of the ligand-centered molecular orbitals with the platinum  $d\pi$  orbitals, which cause delocalization of the molecular orbitals. The shoulder around 420–430 nm could be tentatively assigned to the intraligand charge transfer transition ( ${}^1\text{ILCT}$ ) from the phenylethynylfluorenyl component to the phenanthroline component. Similar spectral feature and assignment have been reported by Che's and our groups for platinum(II) complexes containing fluorene unit [9,10]. The broad, moderately

intense absorption bands in the visible region, i.e. 450–550 nm, likely arise from the metal-to-ligand charge transfer ( ${}^1\text{MLCT}$ ) transitions. For all complexes, there appears to be two distinct bands in this region, indicating two orbitally distinct MLCT transitions due to unequal interaction of the ligand field with the participating Pt  $d$ -orbitals of different symmetry. Similar feature has been reported by Schanze's group for diimine Pt(II) bis-acetylide complexes [22] and by our group for Pt(II) terpyridyl acetylide complexes [23]. It is interesting to note that although the auxiliary substituent at the phenylethynyl motif exhibits a minor effect on the transition energy of the Pt(II) complexes, the molar extinction coefficients of these complexes are influenced significantly by the nature of the substituent. Electron-withdrawing substituent, such as  $\text{NO}_2$ , significantly enhances the molar extinction coefficient of the complex; while electron-donating substituent like  $\text{OCH}_3$  decreases the  $\varepsilon$  values remarkably.

The effect of solvent polarity on the UV–Vis absorption spectra of complexes **5a–5c** was investigated and the results are displayed in Fig. 2 and Supporting information Figs. S1–S3. As exemplified in Fig. 2 for complex **5d**, the absorption bands are bathochromically shifted in less polar solvents, such as in toluene, compared to those in more polar solvents, i.e.  $\text{CH}_3\text{CN}$  and  $\text{CH}_2\text{Cl}_2$ . This negative solvatochromic effect indicates that the dipole moment of the ground state is larger than that of the excited state, which is in line with many other Pt(II)  $\text{C}^{\wedge}\text{N}^{\wedge}\text{N}$  complexes [1a,1,9,24] and Pt(II) terpyridyl complexes reported in the literature [23]. For Pt(II) chloride complexes bearing  $\text{C}^{\wedge}\text{N}^{\wedge}\text{N}$  ligand, the largest dipoles are located around the Pt–Cl and Pt–C bonds due to the negative charges on Cl and C. When the molecule is excited, ligand-to-ligand charge transfer from Cl to phenanthroline and intraligand charge transfer from fluorenyl component to phenanthroline occur. The transition dipoles correlated would cancel the Pt–Cl and Pt–C bond dipoles, which reduces the dipole moment of the excited state. In polar solvent, the more polar ground state is stabilized more than the less polar excited state, therefore the energy gap between the excited state and ground state increases. This causes the blue-shift of the UV–Vis absorption spectrum.

### 3.2. Emission

The emission characteristics of complexes **5a–5d** in a variety of solvents, at different concentrations in  $\text{CH}_2\text{Cl}_2$  at room temperature, and in butyronitrile glassy matrix at 77 K were investigated. All complexes are emissive in solutions at room temperature and in glassy matrix at 77 K. The typical emission spectra in different solvents are provided in Fig. 3a and in Supporting information Figs. S4–S6. The emission lifetimes and quantum yields are summarized in Table 1.

As exemplified in Fig. 3a for complex **5a**, upon excitation at the MLCT band in  $\text{CH}_2\text{Cl}_2$ , a structured emission appears at 624 and 680 nm. The vibronic spacing is approximately  $1320$   $\text{cm}^{-1}$ , which falls in the ring breathing mode of the aromatic rings. The lifetime of the emission is approximately  $7.0$   $\mu\text{s}$ . In view of the large Stokes shift of the emission and the long lifetime, the emission from **5a** at room temperature should originate from a triplet excited state. The vibronic structure in the emission spectrum and the long lifetime suggest that the emission should originate from the  ${}^3\pi,\pi^*$  state, but possibly admixes some  ${}^3\text{MLCT}$  character in view of the negative solvatochromic effect shown in Fig. 3a. The emission spectra of the other three complexes are exactly the same as that for **5a** (Supporting information Fig. S7), with a slightly different emission lifetime and quantum yield (Table 1). The minor effect of the auxiliary substituent at the phenylethynyl motif on the emission suggests that the emitting excited state should be localized on the 2-fluorenyl-1,10-phenanthroline motif.

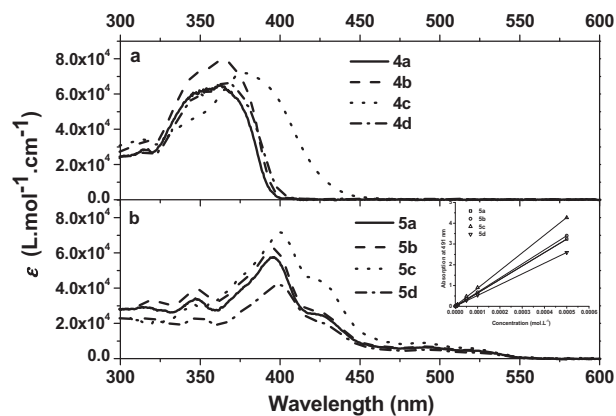
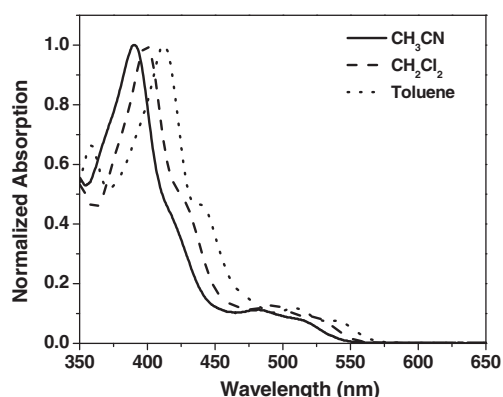


Fig. 1. (a) UV–Vis absorption of ligands **4a–4d** in  $\text{CH}_2\text{Cl}_2$ . (b) UV–Vis absorption spectra of complexes **5a–5d** in  $\text{CH}_2\text{Cl}_2$ , inset shows the linear fitting of the absorbance vs. concentration at 491 nm for **5a–5d**.

**Table 1**  
Photophysical parameters for **5a–5d**.

	$\lambda_{\text{abs}}/\text{nm}^a$ ( $\epsilon/10^3 \text{ L mol}^{-1} \text{ cm}^{-1}$ )	$\lambda_{\text{em}}/\text{nm}^b$ ( $\tau_0/\mu\text{s}; k_q/\text{L mol}^{-1} \text{ s}^{-1}$ ); $\Phi_{\text{em}}$ R.T.	$\lambda_{\text{em}}/\text{nm}^c$ ( $\tau_{\text{em}}/\mu\text{s}$ ) 77 K	$\lambda_{\text{T1-Tn}}/\text{nm}^d$ ( $\tau_{\text{TA}}/\mu\text{s}; \epsilon_{\text{T1-Tn}}/\text{L mol}^{-1} \text{ cm}^{-1}$ ; $\Phi_{\text{T}}$ )
<b>5a</b>	347 (34.2), 396 (57.7), 424 (25.1), 491 (6.39), 524 (4.3)	624 (7.18; $7.24 \times 10^8$ ), 680 (6.98; $6.80 \times 10^8$ ); 0.091	610 (10.9), 668 (10.9)	435 (5.64; 26270; 0.39), 590 (5.46; 48960; 0.39)
<b>5b</b>	348 (39.2), 396 (62.4), 424 (26.9), 490 (6.84), 522 (4.73)	624 (7.19; $8.28 \times 10^8$ ), 680 (7.10; $8.00 \times 10^8$ ); 0.052	610 (10.7), 668 (11.2)	450 (4.55; 24170; 0.44), 620 (6.26; 37840; 0.44)
<b>5c</b>	347 (30.5), 400 (71.8), 424 (44.4), 487 (9.10), 522 (5.82)	624 (5.63; $8.89 \times 10^8$ ), 680 (5.72; $7.48 \times 10^8$ ); 0.079	612 (11.2), 670 (11.6)	462 (5.10; 29310; 0.53), 666 (5.01, 29312, 0.53)
<b>5d</b>	34.8 (23.1), 399 (41.9), 424 (24.8), 492 (5.04), 523 (3.32)	624 (7.26; $7.48 \times 10^8$ ), 680 (7.44; $6.83 \times 10^8$ ); 0.059	612 (9.20), 670 (9.24)	454 (6.42, 29207, 0.51), 654 (5.94, 32858, 0.51)

<sup>a</sup> In  $\text{CH}_2\text{Cl}_2$  solution.<sup>b</sup> Measured at a concentration  $1 \times 10^{-5}$  mol/L in  $\text{CH}_2\text{Cl}_2$  solution.  $\tau_0$  is the intrinsic lifetime at infinite dilute concentration,  $k_q$  is the self-quenching rate constant.<sup>c</sup> Measured at a concentration  $1 \times 10^{-5}$  mol/L in  $\text{CH}_3\text{CH}_2\text{CH}_2\text{CN}$  glassy matrix.<sup>d</sup> In degassed toluene solution.**Fig. 2.** Normalized absorption spectra of **5d** in different solvents at room temperature.

The concentration-dependency emission at room temperature was studied for complexes **5a–5d** in  $\text{CH}_2\text{Cl}_2$ , the results are shown in Fig. 3b for complex **5a** and in Supporting information Figs. S8–S10 for the other three complexes. The emission intensity of each complex increases in the concentration range of  $1 \times 10^{-6}$ – $1 \times 10^{-5}$  mol/L, but decreases when the concentration is higher than  $1 \times 10^{-5}$  mol/L. However, the lifetime keeps decreasing with increased concentration. Therefore, self-quenching clearly occurs for all complexes in the concentration range studied. The self-quenching rate constant and the intrinsic lifetime can be deduced from the slope and the intercept of the Stern–Volmer plot (exemplified in inset of Fig. 3b and in Supporting information Fig. S11 for **5a**), which was described in the experimental section. The

intrinsic lifetime ( $\tau_0$ ) of complex **5a** is thus obtained to be  $\sim 7.2 \mu\text{s}$ , and  $k_q$  to be  $7.24 \times 10^8 \text{ L mol}^{-1} \text{ s}^{-1}$  when monitored at 624 nm. The  $\tau_0$  and  $k_q$  for the other three complexes are listed in Table 1. The  $k_q$  values for these complexes are in line with the values reported for other  $\text{C}^{\wedge}\text{N}^{\wedge}\text{N}$  Pt complexes [9] and for Pt terpyridyl complexes [25].

It should be noted that at the lowest concentration of  $1 \times 10^{-6}$  mol/L, a broad, weak emission band at ca. 490 nm was observed when excited around 400 nm. This band is more salient for **5a** (Fig. 3b) than for the other complexes. Considering the short lifetime of this emission band ( $< 5$  ns), we attribute it to the fluorescence of the coordinated ligand. The possibility of this band being from the free ligand impurity can be ruled out because the respective free ligand exhibits a structured fluorescence at  $\sim 400$ – $415$  nm in dichloromethane (Supporting information Fig. S12) with a lifetime of 960 ps for **4a**. The red-shift of this band with respect to that of the free ligand should be the result of electron delocalization through interaction with the Pt  $d\pi$  orbital. The disappearance of this band at higher concentrations is caused by the inner filter effect considering the remarkable electronic absorption at the excitation wavelength.

In addition, the emission spectra of the ligands and complexes in butyronitrile matrix at 77 K were investigated (Supporting information Figs. S13 and S14). For all of the ligands, the emission spectra at 77 K exhibit clear vibronic structures but remain the same energy as those at room temperature, thus the observed emission is considered as low-temperature fluorescence. When excess amount of iodoethane ( $\text{CH}_3\text{CH}_2\text{I}$ ) was added to the glassy solution, very weak phosphorescence from 525 to 650 nm was observed in addition to the fluorescence signal. The emission spectra of complexes **5a–5d** at 77 K become narrower and slightly blue-shifted compared to those at room temperature (as exemplified in

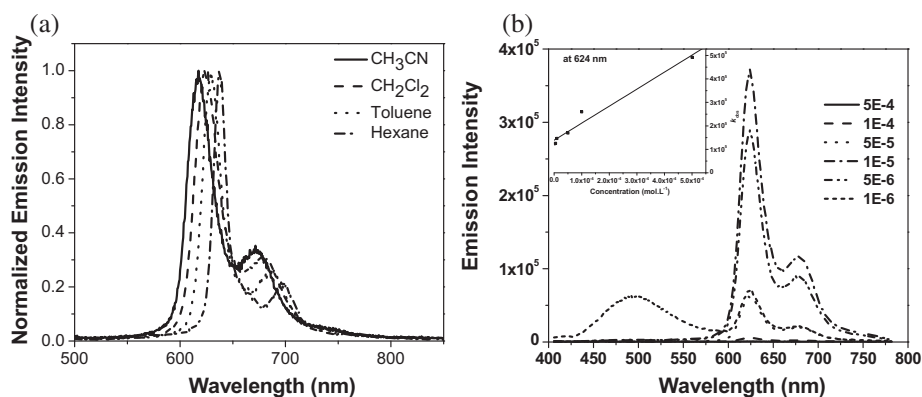
**Fig. 3.** (a) Normalized emission spectra of **5a** in different solvents at room temperature.  $\lambda_{\text{ex}} = 436$  nm; (b) Concentration-dependency emission of **5a** in  $\text{CH}_2\text{Cl}_2$  at room temperature.  $\lambda_{\text{ex}} = 396$  nm. The inset shows the Stern–Volmer fitting result at  $\lambda = 624$  nm.

Fig. S14 for **5a**), which is due to the rigidochromic effect [26]. The vibronic spacing is approximately  $1420\text{ cm}^{-1}$ . Considering the small thermally induced Stokes shift, the similar shape and vibronic spacing of the spectra at 77 K and at room temperature for complexes **5a–5d**, the emission of these Pt complexes at 77 K is assigned to the intraligand  ${}^3\pi,\pi^*$  as well.

### 3.3. Transient absorption

Transient difference absorption (TA) spectroscopy is a useful technique to understand the triplet excited state characteristics. It measures the absorption difference between the ground state and the excited state. A negative band, namely bleaching band, indicates that the ground-state absorption is stronger than that of the excited state, while a positive transient absorption band is *vice versa*. To reveal whether **5a–5d** exhibit triplet excited-state absorption, the triplet TA spectra of these four complexes have been measured using Edinburgh LP920 laser flash photolysis spectrometer, in which the excitation beam is 355 nm from a Quantum Brilliant 4.1 ns laser.

Fig. 4a illustrates the time-resolved TA spectra of complex **5a** in degassed toluene solution. The other three complexes exhibit similar TA spectra (Fig. 4b). All complexes exhibit two broad positive absorption bands from 425 nm to 820 nm, with a bleaching band occurring between 370 and 425 nm, which coincides with the  ${}^1\pi,\pi^*$  transition band in the UV–Vis absorption spectrum. This suggests that the transient absorption likely originates from the  ${}^3\pi,\pi^*$  excited state. All the TA decays monoexponentially throughout the whole spectral range, indicating that the transient absorption arises from the same excited state. Additionally, the lifetime deduced from the decay of the TA and from the decay of the emission are essentially the same, suggesting that the TA could arise from the same excited state that emits, or a state that is in equilibrium with the emitting state.

It should be noted that the TA signals of **5a** at wavelengths above 750 nm go negative at longer decay time. Two factors could be accounted for this. First, the TA signal at longer decay time is very weak, the accuracy of the measurement becomes problematic. Thus the observed negative signal could be an artifact of the experiment. Secondly, the sample solution exhibits minor degradation after several hundreds of laser excitation, which could also contribute to the negative signal.

### 3.4. Reverse saturable absorption (RSA)

As discussed above, complexes **5a–5d** possess long-lived triplet excited states and exhibit broad positive triplet transient absorption. Therefore, reverse saturable absorption is expected to occur

in the positive absorption spectral region. To demonstrate this, nonlinear transmission measurement was conducted for **5a–5d** in  $\text{CH}_2\text{Cl}_2$  solution at 532 nm using 4.1 ns laser pulses. To compare the degree of RSA under the same excitation condition, all the complex solutions were adjusted to an identical linear transmission of 80% at 532 nm in a 2-mm cuvette. As shown in Fig. 5, complexes **5a–5d** exhibit very weak transmission decrease, i.e. very weak RSA, with increased incident fluence. The degree of RSA for these four complexes differs slightly, with **5c** that bears nitro substituent exhibiting the strongest RSA. It seems that electron-withdrawing substituent slightly enhances the RSA, while electron-donating substituent reduces the RSA. As discovered from our previous studies on other platinum complexes, the degree of RSA is mainly determined by the ratio of the excited-state absorption cross-section ( $\sigma_{\text{ex}}$ ) relative to that of the ground state ( $\sigma_{\text{g}}$ ). Although complexes **5a–5d** exhibit a broad and moderately strong triplet transient absorption in the visible to the near-IR region, their ground-state absorption cross sections at 532 nm are relatively large, which are between  $1.07 \times 10^{-17}$  and  $1.58 \times 10^{-17}\text{ cm}^2$ . On the other hand, 532 nm lies almost at the valley of the TA spectra, suggesting that the excited-state absorption of these complexes at 532 nm is quite weak. Both factors lead to reduced ratios of  $\sigma_{\text{ex}}/\sigma_{\text{g}}$ . As a result, the RSA of these complexes becomes very weak. However, the RSA of these complexes could possibly become stronger at longer wavelengths (>550 nm), where the ground-state absorption decreases but the excited-state absorption increases. This needs to be studied in the future when a tunable ns laser is available in our laboratory.

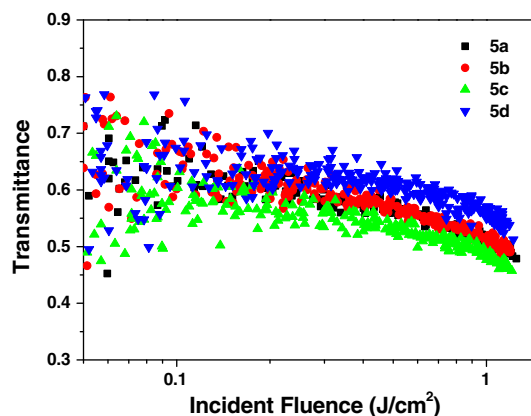


Fig. 5. Nonlinear transmission of complexes **5a–5d** in  $\text{CH}_2\text{Cl}_2$  solution for 4.1 ns laser pulses at 532 nm. The linear transmission is 80%, and the path length of the cuvette is 2 mm. The solution concentration in this study is  $1.46 \times 10^{-4}\text{ mol/L}$  for **5a**,  $1.36 \times 10^{-4}\text{ mol/L}$  for **5b**,  $1.18 \times 10^{-4}\text{ mol/L}$  for **5c**, and  $1.73 \times 10^{-4}\text{ mol/L}$  for **5d**.

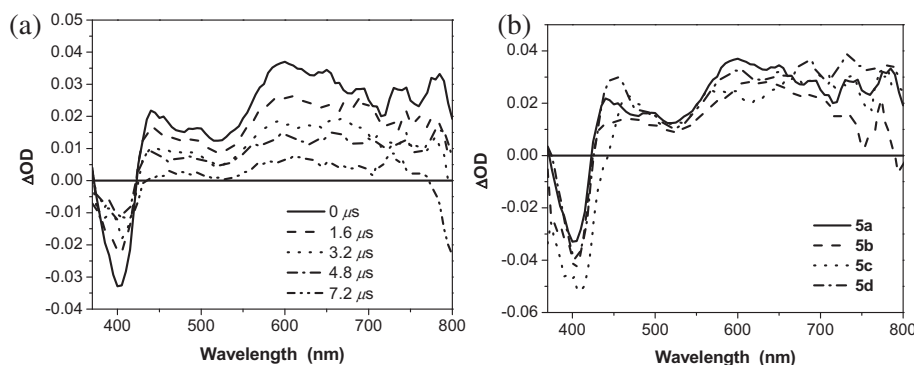


Fig. 4. (a) Time-resolved transient difference absorption spectra of **5a** in degassed toluene solution.  $\lambda_{\text{ex}} = 355\text{ nm}$ . (b) Triplet transient different absorption spectra of **5a–5d** in degassed toluene solution at zero time delay following 355 nm excitation. For all measurements,  $A_{355\text{nm}} = 0.4$  in a 1-cm cuvette.

Another point worthy of mention is that the nonlinear transmission experiments were conducted at high concentration solutions, i.e.  $1.46 \times 10^{-4}$  mol/L for **5a**,  $1.36 \times 10^{-4}$  mol/L for **5b**,  $1.18 \times 10^{-4}$  mol/L for **5c**, and  $1.73 \times 10^{-4}$  mol/L for **5d**. According to the concentration-dependency emission study discussed before, a significant self-quenching occurs at such a high concentration, which reduces the triplet excited-state lifetime drastically. Using the intrinsic lifetime ( $\tau_0$ ) and self-quenching rate constant ( $k_q$ ) listed in Table 1 and the Stern–Volmer Eq. (1), the triplet excited-state lifetime is estimated to be 4.09  $\mu$ s for **5a**, 3.97  $\mu$ s for **5b**, 3.54  $\mu$ s for **5c**, and 3.74  $\mu$ s for **5d** at the respective concentration used for the nonlinear transmission measurement. Although these lifetimes are shorter than the intrinsic lifetimes, they are still much longer than the laser pulse width (4.1 ns) used for the nonlinear transmission study. Therefore, the effect of self-quenching on the excited-state absorption should not be significant. Consequently, the weak RSA observed for these complexes should be predominantly attributed to the small ratio of  $\sigma_{ex}/\sigma_g$  at 532 nm.

#### 4. Conclusion

The platinum(II) complexes bearing 2-(7-(4-*R*-phenylethynyl)-9,9-dihexadecyl-fluoren-2-yl)-1,10-phenanthroline ligand exhibit ligand-centered  $^1\pi,\pi^*$  in the UV and blue region, a  $^1$ ILCT absorption band at ca. 425 nm, and broad  $^1$ MLCT absorption bands in the visible region. The emission of the four complexes is dominated by  $^3\pi,\pi^*$  character, possibly mixed with some  $^3$ MLCT character. The auxiliary substituent on the phenylethynyl motif exhibits negligible effect on the electronic absorption and emission energies of the complexes, indicating that the electron distribution of the frontier molecular orbitals are localized on the ethynyl fluorenylphenanthroline component. All complexes possess long-lived  $^3\pi,\pi^*$  excited state, which gives rise to moderate emission and broadband transient absorption. However, due to their relatively strong ground-state absorption at 532 nm, the RSA of these complexes for nanosecond laser pulse is very weak at 532 nm. Nonetheless, the RSA of these complexes could be stronger at wavelengths longer than 550 nm, in view of the reduced ground-state absorption but increased excited-state absorption at the longer wavelengths.

#### Acknowledgments

This work is partially supported by National Science Foundation (CAREER CHE-0449598) and partially by the Army Research Laboratory (W911NF-06-2-0032 and W911NF-10-2-0055). We are also grateful to Barry Pemberton and Professor Sivaguru Jayaraman at North Dakota State University for measuring the fluorescence lifetimes for ligands **4a–4d**.

#### Appendix A. Supplementary material

Supplementary data associated with this article can be found, in the online version, at <http://dx.doi.org/10.1016/j.ica.2012.03.033>.

#### References

- [1] (a) J. Kalinowski, V. Fattori, M. Cocchi, J.G. Williams, *Coord. Chem. Rev.* 255 (2011) 2401; (b) J.G. Williams, S. Develay, D.L. Rochester, L. Murphy, *Coord. Chem. Rev.* 252 (2008) 2596; (c) W. Lu, B. Mi, M.C.W. Chan, Z. Hui, C. Che, N. Zhu, S. Lee, *J. Am. Chem. Soc.* 126 (2004) 4958; (d) W. Wong, Z. He, S. So, K. Tong, Z. Lin, *Organometallics* 24 (2005) 4079; (e) H. Yersin, D. Donges, W. Humbs, J. Strasser, *Inorg. Chem.* 41 (2002) 4915; (f) S. Chan, M.C.W. Chan, Y. Wang, C. Che, K. Cheung, N. Zhu, *Chem. Eur. J.* 7 (2001) 4180.
- [2] (a) T.J. Wada, S. Chakraborty, R.J. Lachicotte, Q. Wang, R. Eisenberg, *Inorg. Chem.* 44 (2005) 2628; (b) S. Chakraborty, T.J. Wadas, H. Hester, R. Schmehl, R. Eisenberg, *Inorg. Chem.* 44 (2005) 6865;
- (c) E.C. Kwok, M. Chan, K.M. Wong, W.H. Lam, V.W. Yam, *Chem. Eur. J.* 16 (2010) 12244.
- [3] (a) K. Sakai, H. Ozawa, *Coord. Chem. Rev.* 251 (2007) 2753; (b) R. Okazaki, S. Masaoka, K. Sakai, *Dalton Trans.* (2009) 6127; (c) M. Ogawa, G. Ajayakumar, S. Masaoka, H. Kraatz, K. Sakai, *Chem. Eur. J.* 17 (2011) 1148; (d) S. Masaoka, Y. Mukawa, K. Sakai, *Dalton Trans.* (2010) 5868; (e) K. Yamauchi, S. Masaoka, K. Sakai, *J. Am. Chem. Soc.* 131 (2009) 8404; (f) X. Wang, S. Goeb, Z. Ji, N.A. Pogulaichenko, F.N. Castellano, *Inorg. Chem.* 50 (2011) 705; (g) P. Du, J. Schneider, F. Li, W. Zhao, U. Patel, F.N. Castellano, R. Eisenberg, *J. Am. Chem. Soc.* 130 (2008) 5056.
- [4] (a) V. Guercis, J. Fillaut, *Coord. Chem. Rev.* 255 (2011) 2448; (b) K.M. Wong, V.W. Yam, *Coord. Chem. Rev.* 251 (2007) 2477; (c) I. Mathew, W. Sun, *Dalton Trans.* 39 (2010) 5885; (d) H. Zhang, B. Zhang, Y. Li, W. Sun, *Inorg. Chem.* 48 (2009) 3617; (e) Z. Ji, Y. Li, W. Sun, *J. Organomet. Chem.* 694 (2009) 4140; (f) K.M. Wong, W. Tang, X. Lu, N. Zhu, V.W. Yam, *Inorg. Chem.* 44 (2005) 1492; (g) Q. Yang, L. Wu, H. Zhang, B. Chen, Z. Wu, L. Zhang, C. Tung, *Inorg. Chem.* 43 (2004) 5195; (g) W. Lu, M.C.W. Chan, N. Zhu, C. Che, Z. He, K. Wong, *Chem. Eur. J.* 9 (2003) 6155.
- [5] (a) G. Zhou, W. Wong, *Chem. Soc. Rev.* 40 (2011) 2541; (b) R. Liu, Y.J. Li, Y.H. Li, H. Zhu, W. Sun, *J. Phys. Chem. A* 114 (2010) 12639; (c) J. Yi, B. Zhang, P. Shao, Y. Li, W. Sun, *J. Phys. Chem. A* 114 (2010) 7055; (d) W. Sun, B. Zhang, Y. Li, T.M. Pritchett, Z. Li, J.E. Haley, *Chem. Mater.* 22 (2010) 6384; (e) W. Sun, Y. Li, T.M. Pritchett, Z. Ji, J.E. Haley, *Quantum Optics: Concepts in Modern Optics* 40 (2010) 163.
- [6] (a) I. Eryazici, C.N. Moorefield, G.R. Newkome, *Chem. Rev.* 108 (2008) 1834; (b) J.A.G. Williams, *Top. Curr. Chem.* 281 (2007) 205; (c) J.R. Berenguer, E. Lalinde, M.T. Moreno, *Coord. Chem. Rev.* 254 (2010) 832; (d) S.D. Cummings, *Coord. Chem. Rev.* 253 (2009) 449; (e) W. Paw, S.D. Cummings, M.A. Mansour, W.B. Connick, D.K. Geiger, R. Eisenberg, *Coord. Chem. Rev.* 171 (1998) 125; (f) R. McGuire Jr., M.C. McGuire, D.R. McMillin, *Coord. Chem. Rev.* 254 (2010) 2574.
- [7] (a) S. Lai, H. Lam, W. Lu, K. Cheung, C. Che, *Organometallics* 21 (2002) 226; (b) S. Lai, M.C. Chan, K. Cheung, C. Che, *Organometallics* 18 (1999) 3327; (c) S. Diring, P. Retaillieu, R. Ziessel, *J. Org. Chem.* 72 (2007) 10181; (d) J. Schnelder, P. Du, P. Jarosz, T. Lazarides, X. Wang, W.W. Brennessel, R. Eisenberg, *Inorg. Chem.* 48 (2009) 4306; (e) J. Schnelder, P. Du, S. Wang, W.W. Brennessel, R. Eisenberg, *Inorg. Chem.* 48 (2009) 1498.
- [8] G.S. Tong, C. Che, *Chem. Eur. J.* 15 (2009) 7225.
- [9] P. Shao, Y. Li, J. Yi, T.M. Pritchett, W. Sun, *Inorg. Chem.* 49 (2010) 4507.
- [10] M. Yuen, S.C.F. Kui, K. Low, C. Kwok, S.S. Chui, C. Ma, N. Zhu, C. Che, *Chem. Eur. J.* 16 (2010) 14131.
- [11] (a) A. Bencini, V. Lippolis, *Coord. Chem. Rev.* 254 (2010) 2906; (b) H. Chao, Z. Qiu, L. Cai, H. Zhang, X. Li, K. Wong, L. Ji, *Inorg. Chem.* 42 (2003) 8823; (c) K.K. Lo, K.H. Tsang, W. Hui, N. Zhu, *Inorg. Chem.* 44 (2005) 6100; (d) V. Kalsani, M. Schmittel, *Inorg. Chem.* 45 (2006) 2061; (e) J.M. Hamilton, J.R. Whitehead, N.J. Williams, M.E. Ojaimi, R.P. Thummel, R.D. Hancock, *Inorg. Chem.* 50 (2011) 3785.
- [12] (a) C. Girardot, G. Lemerrier, J.C. Mulatier, J. Chauvin, P.L. Baldeck, C. Andraud, *Dalton Trans.* (2007) 3421; (b) C. Girardot, G. Lemerrier, J.C. Mulatier, C. Andraud, J. Chauvin, P.L. Baldeck, *Tetrahedron Lett.* 49 (2008) 1753.
- [13] E.C. Riesgo, X. Jin, R.P. Thummel, *J. Org. Chem.* 61 (1996) 3017.
- [14] A. Picot, C. Feuvrie, C. Barsu, F. Malvoti, B.L. Guennic, H.L. Bozec, C. Andraud, L. Toupet, O. Maury, *Tetrahedron* 64 (2008) 399.
- [15] Y. Hu, M. Wilson, R. Zong, C. Bonnefous, D.R. McMillin, P.R. Thummel, *Dalton Trans.* (2005) 354.
- [16] G.A. Crosby, J.N. Demas, *J. Phys. Chem.* 75 (1971) 991.
- [17] J. Van Houten, R.J. Watts, *J. Am. Chem. Soc.* 98 (1976) 4853.
- [18] I. Carmichael, G.L. Hug, *J. Phys. Chem. Ref. Data* 15 (1986) 1.
- [19] (a) R. Bensasson, C.R. Goldschmidt, E.J. Land, T.G. Truscott, *Photochem. Photobiol.* 28 (1978) 277; (b) S. Foley, G. Jones, R. Liuzzi, D.J. McGarvey, M.H. Perry, T.G. Truscott, *J. Chem. Soc., Perkin Trans. 2* (2) (1997) 1725; (c) C.V. Kumar, L. Qin, P.K. Das, *J. Chem. Soc., Faraday Trans.* 280 (1984) 783.
- [20] P.A. Firey, W.E. Ford, J.R. Sounik, M.E. Keney, M.A.J. Rodgers, *J. Am. Chem. Soc.* 110 (1988) 7626.
- [21] W. Sun, H. Zhu, P.M. Barron, *Chem. Mater.* 18 (2006) 2602.
- [22] C. EdWhittle, J.A. Weinstein, M.W. George, K.S. Schanze, *Inorg. Chem.* 40 (2001) 4053.
- [23] F. Guo, W. Sun, Y. Liu, K.S. Schanze, *Inorg. Chem.* 44 (2005) 4055.
- [24] P. Shao, Y. Li, W. Sun, *J. Phys. Chem. A* 112 (2008) 1172.
- [25] V.W.W. Yam, R.P.L. Tang, K.M.C. Wong, K.K. Cheung, *Organometallics* 20 (2001) 4476.
- [26] (a) A. Juris, V. Balzani, F. Barigelli, S. Campagna, P. Belser, A. von Zelewsky, *Coord. Chem. Rev.* 84 (1988) 85; (b) S. Lai, M.C.W. Chan, K. Cheung, C. Che, *Inorg. Chem.* 38 (1999) 4262; (c) A.S. Poto, M.K. Itokazu, K.M. Frin, A.O. de T. Patrocinio, N.Y.M. Iha, *Coord. Chem. Rev.* 130 (2006) 13.